EARTHQUAKE ENGINEERING AND STRUCTURAL DYNAMICS, VOL. 25, 149–161 (1996)

AN ANALYSIS OF THE SEISMIC CHARACTERISTICS OF STEEL-JACKETED CIRCULAR BRIDGE COLUMNS

Y. H. CHAI

Department of Civil and Environmental Engineering, University of California, Davis, CA 95616, U.S.A.

SUMMARY

The current approach for seismic retrofit of deficient bridge columns in California involves extensive use of steel jacketing. In this paper, the influence of steel jacketing on the lateral response of circular bridge columns is studied; particularly, the enhancement of the ultimate compressive strain of concrete, the increase in curvature ductility capacity and the increase in lateral stiffness are investigated. The current steel jacket thickness used in California is shown to enhance the ultimate compressive strain of concrete by 4–9 times the spalling strain of unconfined concrete. For larger steel jacket thickness, the ultimate limit state of steel-jacketed columns may be governed by the low-cycle fatigue fracture of the longitudinal reinforcement instead of the ultimate compressive strain of concrete. Steel jacketing is also expected to increase significantly the lateral stiffness of columns if full-height steel jackets are used. The increase in lateral stiffness of flexural columns ($3 \leqslant L/D \leqslant 9$) is estimated to be 35–60 per cent using current jacket thickness. Inelastic dynamic analyses of steel-jacketed columns using ground motions recorded during the 1989 Loma Prieta earthquake indicated that the current steel jacket thickness provides adequate protection against the damage potential of the ground motions with comparable spectral acceleration as that specified in current design spectra, and the damage sustained by the steel-jacketed column is likely to be repairable.

KEY WORDS: bridge retrofit; steel jacketing; reinforced concrete columns; cumulative damage; earthquake hazard mitigation

INTRODUCTION

In the substructure retrofit program implemented by the California Department of Transportation (Caltrans) in the late 1980's, bridge columns with pre-1971 details were identified as particularly vulnerable to earthquake ground motions and were given a high priority for retrofit. Steel jacketing was used extensively for retrofitting of these columns. Experimental studies have shown a significant improvement in the seismic response of steel-jacketed columns over the 'as-built' columns of pre-1971 details with ductility capacity of the column significantly enhanced by the steel jacket.[1,2] The effectiveness of steel jacketing was also evident in the field during the recent 1994 Northridge earthquake. An estimated sixty retrofitted bridges, many of which have been steel jacketed, were located in the region of intense ground shaking with peak ground acceleration exceeding $0{\cdot}25g$.[3] None of the steel-jacketed columns were reported to have sustained any significant damage. As an example, Figure 1(a) shows the good condition of two steel-jacketed columns after the 1994 Northridge earthquake. With the exception of minor spalling of concrete at the connection between the column and superstructure, the steel-jacketed columns survived the ground motion without any significant damage. In contrast, however, two adjacent unretrofitted structures collapsed due to column failures during the 1994 Northridge earthquake. Figure 1(b) shows the collapsed columns for one of the structures. A peak horizontal ground acceleration exceeding $0{\cdot}3g$ has been estimated at the collapsed bridge sites.[4] Although a direct comparison of performance between the retrofitted and collapsed structures in Figure 1 cannot be made due to the possible variation in structural characteristics and ground motions, the excellent condition of the steel-jacketed columns after the earthquake nonetheless points to an effective method for mitigating the risk of bridge collapse due to column failure.

The good performance of steel-jacketed bridge columns during the 1994 Northridge earthquake motivated the study discussed in this paper. The main objectives of the study were to investigate the influence of steel

CCC 0098-8847/96/020149–13

Received 22 April 1995
Revised 22 August 1995

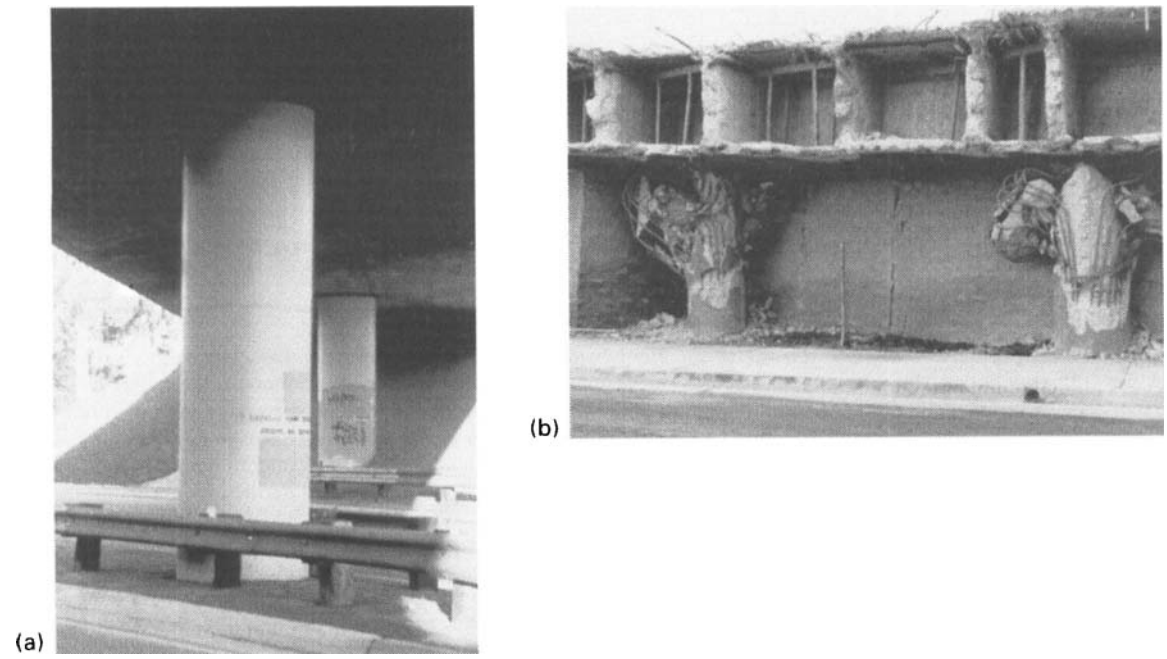

Figure 1. Bridge column performance during the 17 January, 1994 Northridge earthquake (a) Steel Jacketed Columns–Cadillac Street Off-Ramp Structure, Interstate I-10 (b) Non-Ductile Columns–La Cienega-Venice Undercrossing, Interstate I-10

jacketing on the structural characteristics of circular bridge columns. In particular, the increase in lateral stiffness and ductility capacity of the circular column are investigated. The study also included a damage assessment of steel-jacketed columns using ground motions recorded during the 17 October, 1989 Loma Prieta earthquake.

INFLUENCE OF STEEL JACKET ON COLUMN BEHAVIOUR

Ultimate compressive strain

The primary role of a steel jacket is to provide additional confinement to concrete columns that are deficient in transverse reinforcement. Under the combined action of axial compression and bending moment, the compression region of the column dilates as the flexural strength of the member is approached. The dilation of concrete is restrained by the steel jacket resulting in a significant increase in the ultimate compressive strain of concrete. The ultimate compressive strain confined by the steel jacket ε_{cu} can be estimated using the energy balance method:[5,6]

$$\varepsilon_{cu} = \varepsilon_{sp} + 1{\cdot}4\varepsilon_{suj}\rho_{sj}\frac{f_{yj}}{f'_{cc}} \tag{1}$$

where ε_{sp} = spalling strain of the unconfined concrete; ε_{suj} = ultimate tensile strain of the steel jacket; f_{yj} = yield strength of the steel jacket; ρ_{sj} = volumetric confining ratio of the steel jacket, and is defined by

$$\rho_{sj} = 4t_j/(D_j - 2t_j) \tag{2}$$

where t_j = thickness of the steel jacket; and D_j = outside diameter of the steel jacket. The term f'_{cc} in equation (1) corresponds to the confined compressive strength of the concrete which, for a circular column, can be estimated by[5]

$$f'_{cc} = f'_c\left(2{\cdot}254\sqrt{1 + 7{\cdot}94\frac{f'_l}{f'_c}} - 2\frac{f'_l}{f'_c} - 1{\cdot}254\right) \tag{3}$$

where f_c' = unconfined compressive strength of concrete; and f_l' = effective confining pressure of the steel jacket, and is given by

$$f_l' = \tfrac{1}{2}\rho_{sj} f_{yj} \tag{4}$$

The enhancement of ultimate compressive strain of concrete by the steel jacket is significant in current retrofit application. The design jacket thickness currently specified by Caltrans for circular columns is given by[7]

$$t_j = C_j \frac{D}{200} \geqslant 6{\cdot}4 \text{ mm} \tag{5}$$

where D = diameter of column, and C_j = coefficient depending on the details of the longitudinal reinforcement at the base of the column, i.e.

$$C_j = \begin{cases} 1{\cdot}0 & \text{continuous longitudinal reinforcement} \\ 1{\cdot}2 & \text{lapped longitudinal reinforcement} \end{cases} \tag{6}$$

Equations (5) and (6) are intended to provide an effective confining pressure of $f_l' = 2{\cdot}0$ MPa for the concrete. For columns with inadequate lap-splices, e.g. $l_{lap} = 20d_b$, in the longitudinal reinforcement, a 20 per cent increase in jacket thickness is specified in order to prevent bond failure in the lap-splices. The larger steel jacket thickness is intended to limit the circumferential strain of the steel jacket to 1000×10^{-6} instead of the 1200×10^{-6} expected for the yield strain of Grade A36 steel commonly used for steel jacketing in California. For smaller diameter columns, i.e. $D \leqslant 1219$ mm, a minimum jacket thickness of $t_j = 6{\cdot}4$ mm is specified in current retrofit design. The minimum thickness is primarily intended to provide adequate rigidity to the steel jacket for ease of handling and installation of the steel jacket in the field. Although not explicitly specified, a jacket thickness of $t_j = 25$ mm is considered as the practical upper limit in steel jacket application. Note that equations (5) and (6) indicate that the steel jacket thickness ratios currently used for design are 0·005 and 0·006 for columns with continuous and lap-spliced longitudinal reinforcement, respectively. Figure 2 shows the enhancement of the ultimate compressive strain of concrete under various steel jacket thickness ratios t_j/D. A spalling strain of $\varepsilon_{sp} = 0{\cdot}005$ has been assumed for the unconfined concrete, and a yield strength of $f_{yj} = 248$ MPa and an ultimate tensile strain of $\varepsilon_{suj} = 0{\cdot}20$ have been assumed for the steel jacket. It can be seen from Figure 2 that a large increase in ultimate compressive strain is achieved with current steel jacket thickness. For example, the retrofit of a circular column by a jacket thickness ratio of $t_j/D = 0{\cdot}005$ and 0·006

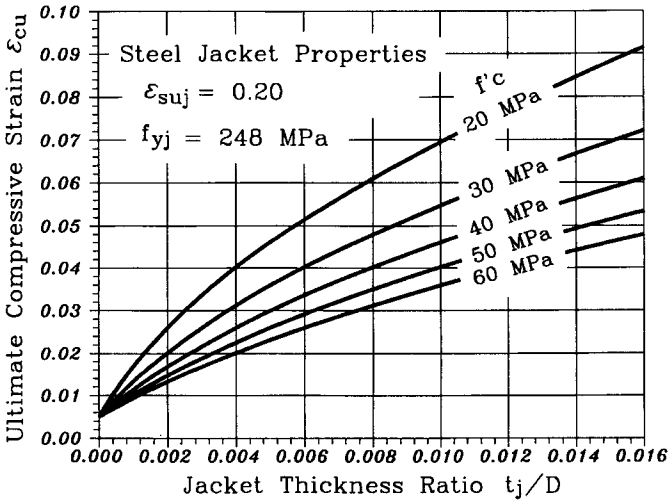

Figure 2. Theoretical enhancement of ultimate compressive strain by steel jacketing

would provide 7·2 and 8·1 times increase in the ultimate compressive strain of concrete for $f_c' = 30$ MPa, respectively. It can also be seen from Figure 2 that the enhancement of ultimate compressive strain decreases with increased concrete strength due to the more brittle nature of higher strength concrete. For instance, using the same jacket thickness ratios of $t_j/D = 0{\cdot}005$ and 0·006, the increase in ultimate compressive strain reduces to 4·6 and 5·2 for a concrete strength of $f_c' = 60$ MPa, respectively.

Moment–curvature response

The enhancement of ultimate compressive strain of concrete by steel jacketing causes a corresponding increase in the curvature ductility capacity of the column. The increase in curvature ductility is accompanied by an increase in the tensile strain of the extreme reinforcement. Depending on the level of confinement provided by the steel jacket, the ultimate limit state of a steel-jacketed column may be governed by the ultimate compressive strain of the concrete, as given by equation (1), or the low-cycle fatigue fracture of the extreme tensile steel.[6] Figure 3 shows a simulation of the moment–curvature response of a circular column with $D = 1500$ mm confined by various steel jacket thickness using the program COLRET.[8] Steel jackets in the range $t_j = 0$ to 25 mm, or $t_j/D = 0$ to 0·0164, were used for the analysis. The longitudinal reinforcement was provided by 25 No. 14 ($d_b = 43$ mm) Grade 40 ($f_y = 276$ MPa) bars and the transverse reinforcement was provided by No. 4 ($d_{bh} = 12{\cdot}7$ mm) Grade 40 ($f_{yh} = 276$ MPa) circular hoops at 305 mm centres. The total area of the longitudinal reinforcement corresponds to 2 per cent of the column cross-sectional area. The yield strength of the steel jacket was $f_{yj} = 248$ MPa. It can be seen from Figure 3 that the initial moment–curvature response was largely unaffected by the presence of the steel jacket. A minimal lateral expansion of the column occurs at early stages of loading and the steel jacket remains essentially inactive. At higher lateral loads however a significant lateral expansion of concrete occurs in the compression region of the column, but spalling of cover concrete is delayed until a much larger curvature ductility is developed. The large increase in curvature ductility capacity due to steel jacketing can be seen in Figure 3 even for small jacket thickness ratios. In this example, the curvature increases from an unconfined curvature ductility factor of $\phi_u/\phi_y' = 10$ to a confined curvature ductility factor of $\phi_u/\phi_y' = 31$ for a jacket thickness of $t_j = 5$ mm, or $t_j/D_j = 0{\cdot}0033$, where ϕ_u, ϕ_y' are ultimate and first-yield curvature, respectively. For intermediate jacket thickness of $t_j = 5$ to 15 mm, or $t_j/D = 0{\cdot}0033$ to 0·0098, the ultimate conditions were limited by the ultimate compressive strain of the concrete, whereas for a larger jacket thickness of $t_j = 20$ and 25 mm, or

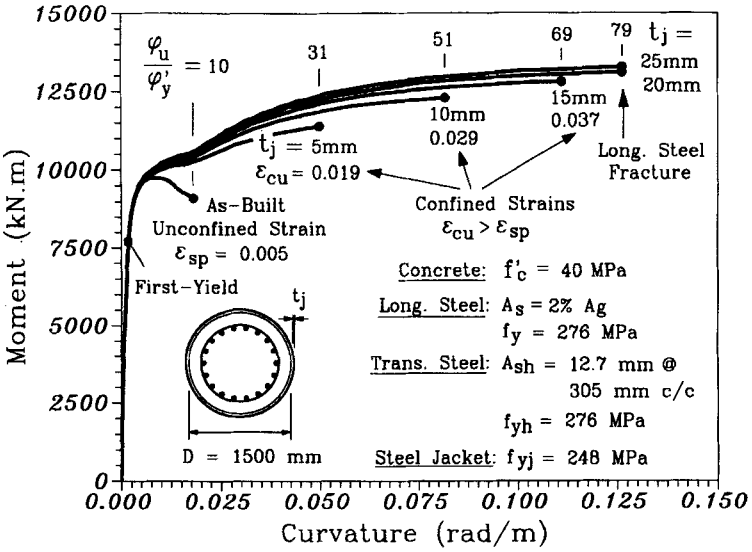

Figure 3. Monotonic moment–curvature response of 'as-built' and steel-jacketed circular sections

$t_j/D = 0{\cdot}0131$ and $0{\cdot}0164$, the ultimate condition was limited by the ultimate tensile strain of the longitudinal steel. Although not apparent in Figure 3, the expected curvature ductility factor for this example using the current design jacket thickness ratio of $t_j/D = 0{\cdot}005$ is $\phi_u/\phi'_y = 41$. Note that the increase in curvature ductility is also accompanied by an increase in the flexural strength, due to strain hardening of the longitudinal steel and the increased compressive strength of concrete as a result of confinement by the steel jacket. The rate of flexural strength increase however decreases with increased steel jacket thickness.

Column lateral stiffness

In addition to enhancing the strength and ductility of a column, the presence of a steel jacket also increases the lateral stiffness of the column. The increase in lateral stiffness may translate into an increase in seismic design force level for the structure.[6] In the encased region of the column, full composite action between the steel jacket and column cannot be realized until a finite bond transfer length is developed. The increase in stiffness due to steel jacketing depends on the thickness and length of the steel jacket and the bond strength between the jacket and column. Laboratory tests on flexural columns ($L/D = 6$) showed a modest increase in lateral stiffness of 10–15% when a steel jacket length of only twice the column diameter was used.[1] On the other hand, tests on shear columns ($L/D = 2$ and $1{\cdot}5$) showed a larger lateral stiffness increase of 23–41% where full-height steel jackets were provided for shear strength enhancement.[2] A common practice in the field however is to use full-height steel jacket regardless of the column aspect ratios in order to provide a uniform appearance to columns after retrofit. In this study, lateral stiffness simulation for flexural columns ($3 \leqslant L/D \leqslant 9$) is made assuming full-height steel jackets. Figure 4 shows the increase in column lateral stiffness as a function of jacket thickness ratio, t_j/D, the bond strength between column and steel jacket, $\bar{u}_0$, and the columns aspect ratio, L/D, where L = effective height of column. The x-axis corresponds to the jacket thickness ratio, and the y-axis corresponds to the ratio of the lateral stiffness of steel jacketed column, k_r, to that of the 'as-built' column, k_0, where the lateral stiffnesses have been defined as:

$$k_r \text{ or } k_0 \equiv \frac{V_y}{\Delta'_y} \tag{7}$$

where V_y = lateral force to cause first-yielding of the longitudinal reinforcement; Δ'_y = lateral displacement at first yield of longitudinal reinforcement. The lateral force and displacement of 'as-built' and steel jacketed columns at first yield of longitudinal reinforcement were estimated using the analytical model presented in Reference 6. A steel jacket thickness ratio in the range of $t_j/D = 0$ to $0{\cdot}0164$, and a bond strength in the range of $\bar{u}_0 = 350$ to 2100 kPa were used in the study. Material properties and column dimensions similar to that used for moment–curvature simulation were used for lateral stiffness simulation. It can be seen from Figure 4 that the increase in lateral stiffness of steel-jacketed columns is fairly sensitive to the increase in bond strength between the jacket and column, even though the rate of increase in lateral stiffness diminishes with increased bond strength. As an example using the current design thickness ratio of $t_j/D = 0{\cdot}005$ and an aspect ratio of $L/D = 3$, a 37 per cent increase in lateral stiffness is expected for a bond strength of $\bar{u}_0 = 700$ kPa, whereas a 46 per cent increase in lateral stiffness is expected for a bond strength of $\bar{u}_0 = 1400$ kPa. In practice, however, a large variation in bond strengths can be expected with values ranging from 150 to 1800 kPa having been reported.[6] A comparison between Figures 4(a)–4(c) also shows that the lateral stiffness of a steel-jacketed column increases with the aspect ratio of the column. For example, using the same design thickness ratio of $t_j/D = 0{\cdot}005$ and a bond strength of $\bar{u}_0 = 1400$ kPa, the lateral stiffness increases from the 46 per cent for $L/D = 3$ to 55 and 59 per cent for $L/D = 6$ and 9, respectively.

DAMAGE ANALYSIS OF STEEL-JACKETED COLUMNS

Ground motions

The expected good seismic performance of steel-jacketed bridge columns is further verified through a series of inelastic dynamic analyses using ground motions recorded during the 17 October, 1989 Loma Prieta earthquake. Figure 5(a) shows the N–S component of the ground acceleration recorded at a rock site at

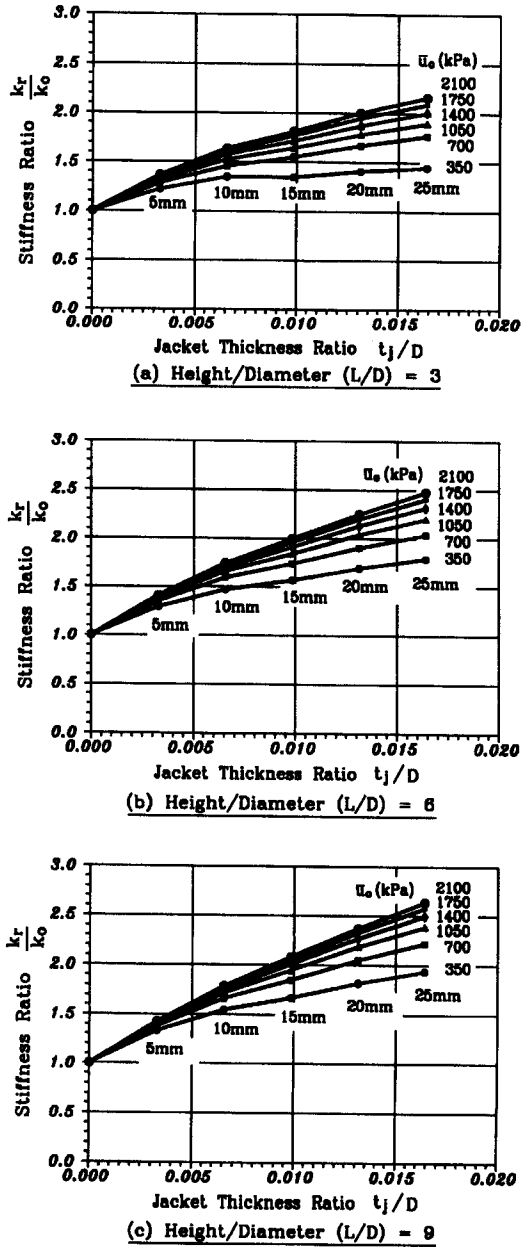

Figure 4. Column lateral stiffness increase due to steel jacketing

Corralitos-Eureka Canyon Road which was located about 5 km from the epicentre, and Figure 5(b) shows the N35° component of the ground acceleration recorded at a soft soil site at the Oakland Outer Harbor Wharf which was located about 65 km from the epicentre. In this study, the ground motion recorded at the Oakland Outer Harbor Wharf had been scaled to the same peak ground acceleration of the Corralitos record, i.e. 0·63*g*. The spectral acceleration of the two ground motions are compared with the design spectrum currently specified by Caltrans[9] in Figure 6. The elastic spectral acceleration of the Corralitos record is plotted against the Caltrans design spectrum specified for a 'rock' site (0–3 m alluvium) in Figure 6(a). The predominant period of the Corralitos record is $T_g \approx 0{\cdot}3$ sec which compares well with the

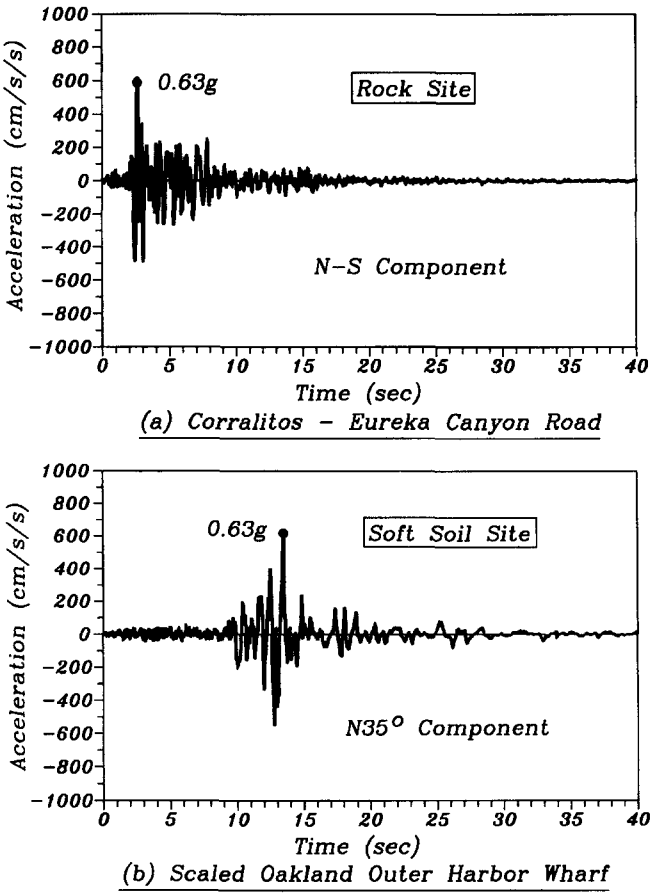

Figure 5. Ground motions recorded during 17 October, 1989 Loma Prieta earthquake

predominant period of the Caltrans design spectrum. The spectral acceleration at the predominant period is about 2·1 g which exceeds the Caltrans design spectrum by about 17 per cent. The spectral acceleration of the Corralitos record also shows a more rapid attenuation with the period of the structure compared to Caltrans design spectrum. The elastic spectral acceleration of the scaled Oakland Outer Harbor Wharf record is plotted against the Caltrans design spectrum specified for a soft soil site (24–48 m alluvium) in Figure 6(b). The predominant period of the Oakland record is about 0·9 sec which is longer than the predominant period of the Caltrans design spectrum of 0·5 sec. The spectral acceleration at the predominant period is 1·67g which also exceeds the Caltrans design spectrum by about 14 per cent.

Structural parameters

Inelastic dynamic analyses of single-circular bridge columns confined by steel jackets of various thickness ratios were carried out using the program NONSPEC.[10] A bilinear stiffness model was used in the analysis which was obtained by linear approximations of the load–deformation curve computed by COLRET.[8] A straight line was used to connect the origin to the point which corresponds to first-yielding of the longitudinal reinforcement, and another line was used to connect the first-yield point to the ultimate limit state of the column. A seismic mass corresponding to an axial stress level of $0{\cdot}1f_c'$ was assumed for the column. Three longitudinal reinforcement area ratios were investigated, namely $A_s = 0{\cdot}01$, 0·02 and $0{\cdot}03A_g$ where A_g = column cross-sectional area, and a column diameter of $D = 1500$ mm was assumed. The transverse reinforcement was provided by No. 4 circular hoops ($d_{bh} = 12{\cdot}7$ mm) at 305 mm centres which is

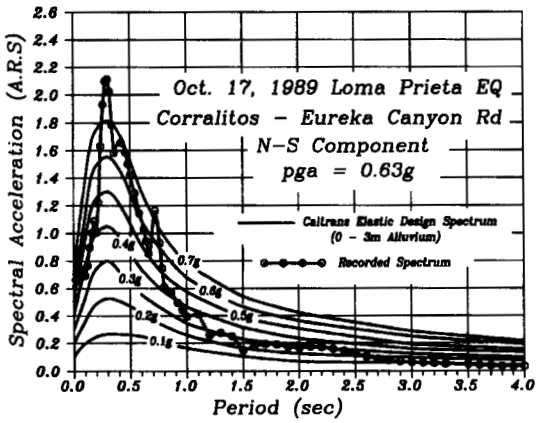

(a) Corralitos - Eureka Canyon Rd N-S Record

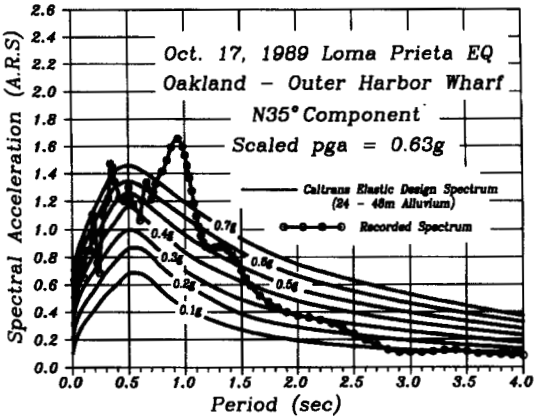

(b) Scaled Oakland - Outer Harbor Wharf N35° Record

Figure 6. Spectral acceleration of ground motions versus Caltrans design spectra

representative of the pre-1971 details in California. Instead of using the nominal yield strength of the reinforcement, the expected mean strength of $f_y = f_{yh} = 336$ MPa for Grade 40 steel had been assumed for the longitudinal and transverse steel. The yield strength of the steel jacket was assumed to be $f_{yj} = 248$ MPa and a bond strength of $\bar{u}_0 = 1400$ kPa was assumed for the steel jacket. Two column aspect ratios were investigated, namely $L/D = 6$ and 3, and these aspect ratios were chosen to give structural periods close to the predominant periods of the ground motions. Figure 7 shows the variation of structural periods with steel jacket thickness $t_j/D = 0$ to 0·0164. It can be seen from Figure 7 that the structural periods of columns with aspect ratio of $L/D = 3$ are slightly larger than the predominant period of the Corralitos record, whereas the structural period of columns with aspect ratio of $L/D = 6$ crosses over the predominant period of the scaled Oakland Outer Harbor Wharf record.

Damage modelling

Structural damage to bridge columns is assessed using the modified Park and Ang model which assumes damage to be a linear combination of normalized peak response displacement and normalized total hysteretic energy dissipated under by the structure during the response:[11,12]

$$D_i = \frac{\Delta_m}{\Delta_{um}} + \frac{\beta^*(E_h - E_{hm})}{V_y \Delta_{um}} \tag{8}$$

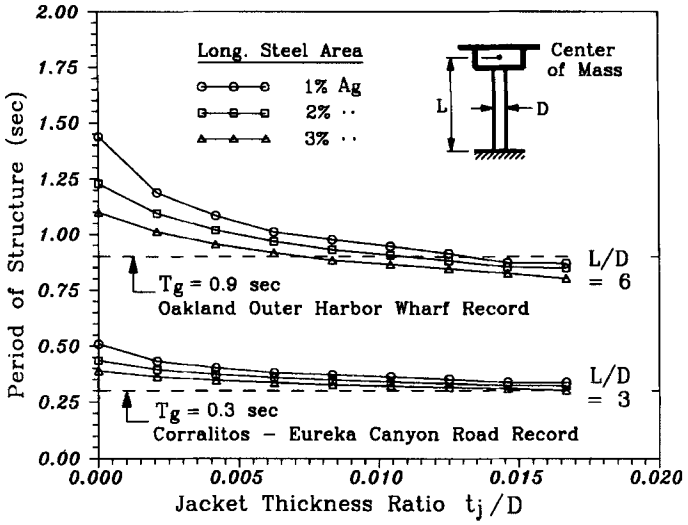

Figure 7. Structural periods versus steel jacket thickness ratios

where Δ_m = peak response displacement; Δ_{um} = ultimate displacement under monotonic loading; V_y = yield strength of the structure; β^* = strength deterioration parameter; E_h = total plastic strain energy dissipated by the structure; and E_{hm} = plastic strain energy dissipated by the structure under a monotonic loading. A damage index of $D_i \geqslant 1$ signifies failure of the structure. Note that, in the modified damage model, i.e. equation (8), only the portion of the plastic strain energy dissipated above that of monotonic loading is considered as contributing to damage. The ultimate displacement of a column under monotonic loading can be estimated by assuming a plastic hinge rotation at the base of the column, i.e.

$$\Delta_{um} = \Delta_y + (\phi_u - \phi_y) L_p (L' - 0{\cdot}5 L_p) \tag{9}$$

where Δ_y = elasto-plastic yield displacement; ϕ_y = elasto-plastic yield curvature; L_p = equivalent plastic hinge length; L' = effective height of column; and ϕ_u = ultimate curvature. The program COLRET[8] calculates the effective height of the column L' by assuming a longitudinal reinforcement strain penetration into the footing to a depth of $0{\cdot}022 f_y d_b$ (second term of equation (10) below) where f_y is the yield strength of the longitudinal reinforcement in MPa units. For the 'as-built' column, i.e. without retrofit, the equivalent plastic hinge length can be estimated by[13]

$$L_p = 0{\cdot}08L + 0{\cdot}022 f_y d_b \tag{10}$$

where d_b = longitudinal bar diameter; L = original height of the column; and f_y = yield strength of the longitudinal reinforcement in MPa units. For retrofitted columns, the radial stiffness of the steel jacket restricts the spread of inelastic curvature up the column resulting in a reduced plastic hinge length. Experimental tests of steel-jacketed columns have indicated a 40 per cent reduction in plastic hinge length for a steel jacket thickness of $t_j/D = 0{\cdot}008$.[1] An expression for the equivalent plastic hinge length of steel-jacketed columns has been proposed:[2]

$$L_p = 0{\cdot}044 f_y d_b + v_g \tag{11}$$

where v_g = vertical gap between the toe of the jacket and the top of footing, and is typically limited to 50 mm or the clear cover of longitudinal reinforcement whichever is smaller; and f_y = yield strength of the longitudinal reinforcement in MPa units. In this study, a linear transition in plastic hinge length between the 'as-built' columns and steel-jacketed column is assumed. As shown in Figure 8, the equivalent plastic hinge length is assumed to decrease linearly from the 'as-built' plastic hinge length, as given by equation (10), to the full-restrained steel jacketed plastic hinge length, as given by equation (11), which is assumed to occur at

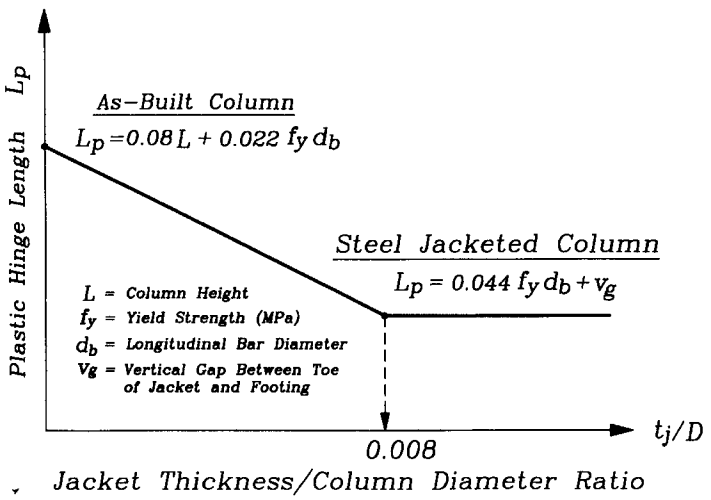

Figure 8. Equivalent plastic hinge length versus steel jacket thickness ratio

a jacket thickness ratio of $t_j/D = 0{\cdot}008$. For steel jacket thickness ratio of $t_j/D > 0{\cdot}008$, the equivalent plastic hinge length is assumed to remain constant as shown in Figure 8.

Analysis results

The damage index for steel-jacketed columns with aspect ratio $L/D = 3$ subjected to the Corralitos–Eureka Canyon Road record is plotted against the steel jacket thickness ratio in Figure 9(a). A strength deterioration parameter of $\beta^* = 0{\cdot}05$ (Reference 6) has been assumed for the damage analyses. It can be seen from Figure 9(a) that a damage index greater than unity was calculated for all the 'as-built' columns. A damage index of $D_i = 1{\cdot}72$ was computed for the 'as-built' column with 1 per cent longitudinal steel area. Although the damage index of the 'as-built' column decreases rather rapidly with the increase in longitudinal steel area, failure was expected in all three columns. The effectiveness of steel jacketing in reducing the damage to columns is clearly evident in Figure 9(a). A rapid decrease in damage index was computed for a relatively small jacket thickness ratio of $t_j/D \leqslant 0{\cdot}004$. The design jacket thickness currently specified by Caltrans is seen to provide adequate protection against the damage potential of the Corralitos record. The computed damage indices were, 0·3 to 0·4, and 0·20 to 0·32, for $t_j/D = 0{\cdot}005$ and 0·006, respectively. The damage index for taller steel-jacketed columns of $L/D = 6$ subjected to the scaled Oakland Outer Harbor Wharf record is shown in Figure 9(b). Damage indices greater than unity were also computed for all three 'as-built' columns and a large damage index of $D_i = 1{\cdot}92$ was computed for the column with 1 per cent longitudinal steel area. The effectiveness of steel jacketing can also be seen in Figure 9(b) where a rapid decrease in damage index was computed for relatively small steel jacket thickness. The current jacket thickness is seen to provide adequate protection against the damage potential of the Oakland record. For a steel jacket thickness larger than that used in current retrofit design, the computed damage indices remain relatively constant for both ground motions.

Experimental correlation

In order to provide a correlation between the physical damage of steel-jacketed columns and the damage model, damage indices were computed at various stages of loading for steel-jacketed columns reported in Reference 1. The length of the steel jacket in these tests was extended to only twice the diameter of the column, and the steel jacket thickness ratio was $t_j/D = 0{\cdot}008$. Figure 10(a) shows the condition of a steel jacketed column after five cycles to a peak lateral force of $0{\cdot}66V_y$ where V_y = yield strength of the column. Only minor flexural cracking were observed above the steel jacket and at the base of the column, and no cracking was noted in the footing. Since yielding of the longitudinal reinforcement did not occur at this stage

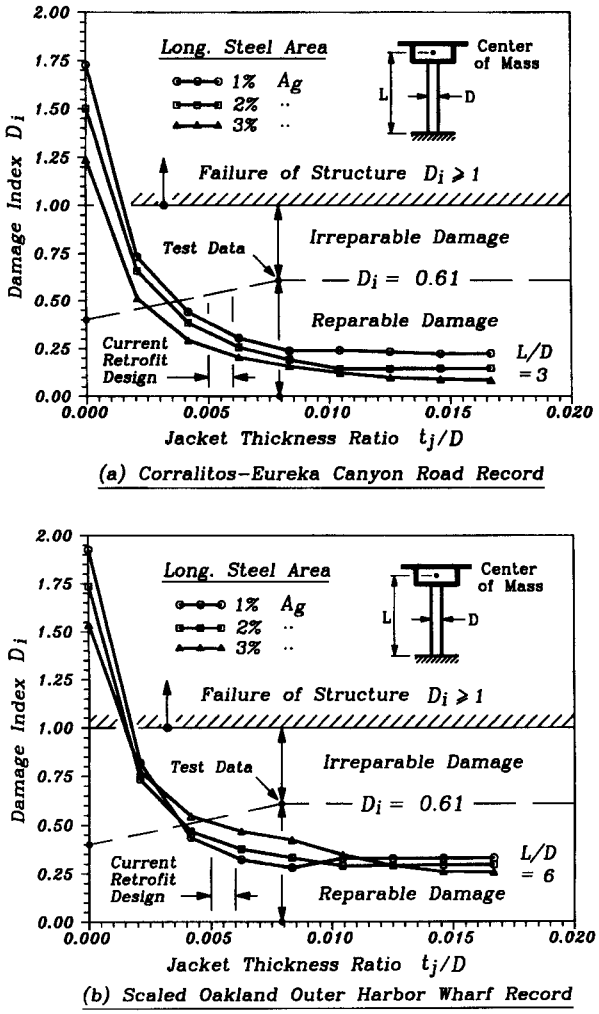

Figure 9. Damage index for steel-jacketed columns subjected to ground motions recorded during the 17 October, 1989 Loma Prieta earthquake

of loading, the column is assumed to be elastic and D_i is taken as zero. Figure 10(b) shows the physical damage of the column at a damage index of $D_i = 0{\cdot}30$ where cracking above the jacket became more extensive and occurred at closer spacing than those observed in Figure 10(a). Minor spalling of cover concrete was also observed at this stage of loading at the base of the column where the steel jacket was terminated. Further loading of the column beyond $D_i = 0{\cdot}30$ caused the inelastic deformation to be concentrated at the base of the column and top of the footing. Figure 10(c) shows the damage stage at $D_i = 0{\cdot}61$ where severe spalling of concrete at the base of column and on top of the footing occurred. The loss of cover concrete from the top of footing led to eventual exposure and buckling of longitudinal reinforcement. Figure 10(d) shows the final failure of the steel-jacketed column with $D_i = 1$ where the longitudinal reinforcement fractured under repeated cycles of compression buckling and reversed tensile straightening. Since repair of buckled reinforcement after an earthquake is generally difficult and expensive, the damage index of $D_i = 0{\cdot}61$ shown in Figure 10(c), after which buckling of reinforcement occurred due to severe spalling of cover concrete from the column and footing, is taken to correspond to the irreparable damage state of steel-jacketed columns. The damage index of $D_i = 0{\cdot}61$ is plotted in Figures 9(a) and 9(b) for the jacket thickness of $t_j/D \geq 0{\cdot}008$. A damage index of $D_i = 0{\cdot}4$, as suggested in Reference 14, is assumed to

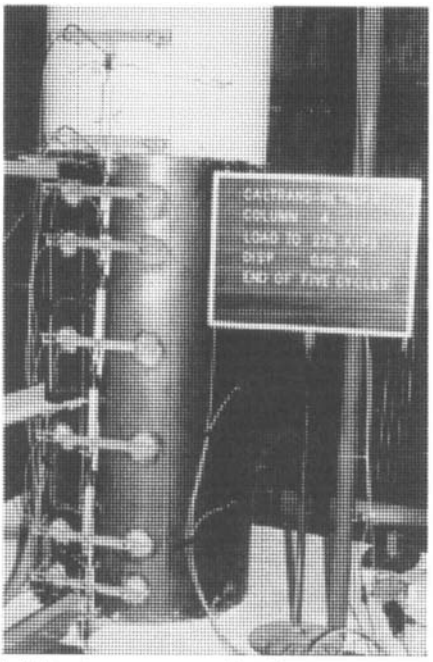

(a) Elastic response – $D_T = 0$

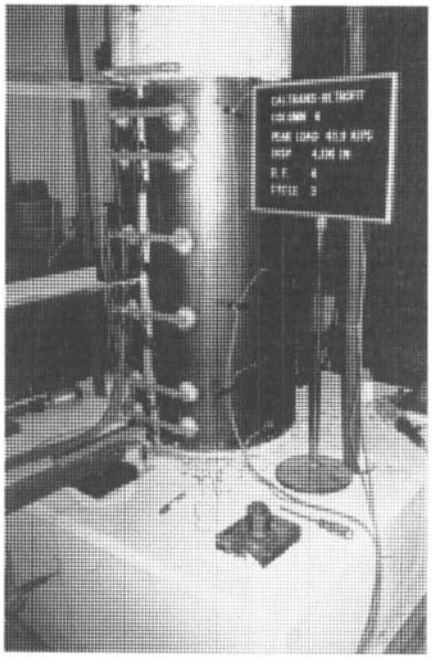

(b) Reparable Damage – $D_T = 0{\cdot}30$

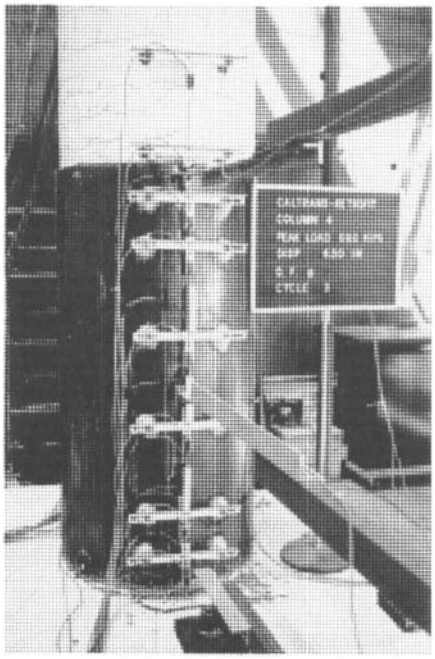

(c) Irreparable Damage – $D_T = 0{\cdot}61$

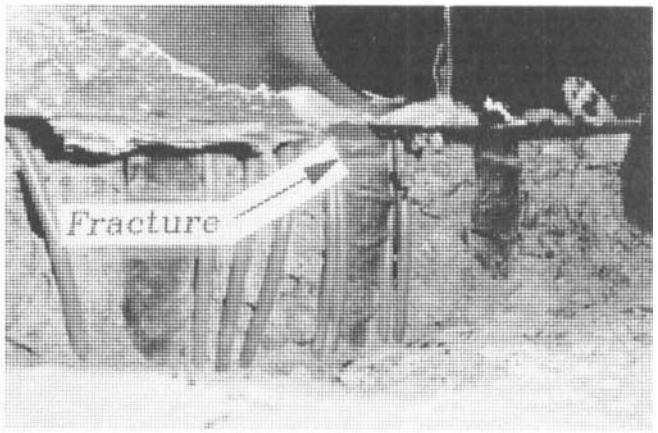

(d) Failure – $D_T = 1{\cdot}00$

Figure 10. Correlation between damage index and observed damage of steel-jacketed column

correspond to the reparable limit of 'as-built' columns in Figures 9(a) and 9(b). A linear line connecting the two points is used to define the reparable limit state of steel-jacketed columns with $t_j/D < 0{\cdot}008$. It can be seen from Figures 9(a) and 9(b) that the physical damage sustained by columns retrofitted with current Caltrans jacket thickness is likely to be reparable when subjected to ground motion with damage potential comparable with current Caltrans design spectra.

CONCLUSIONS

Experimental testing and observations made during the recent 1994 Northridge earthquake have both indicated that steel jacketing is effective in mitigating the risk of bridge collapse due to failure of old bridge columns. The current guideline for steel jacketing of circular columns in California uses a steel jacket thickness ratio of 0·005 and 0·006 for columns with continuous and lap-spliced longitudinal reinforcement, respectively. The current jacket thickness provides a significant enhancement in the ultimate compressive strain of concrete, typically in the range 4–9 times the spalling strain of unconfined concrete. The increase in ultimate compressive strain of concrete is accompanied by a large increase in curvature ductility of the column as well as the tensile strain of the extreme reinforcement. A possible ultimate limit state exists, particularly for large jacket thicknesses, where failure of steel jacketed columns may be governed by fracture of the longitudinal reinforcement instead of the ultimate compressive strain of the concrete. Steel jacketing can also be expected to cause a significant increase in the lateral stiffness of the column if full-height well bonded steel jackets are used. The increase in lateral stiffness increases with the column aspect ratio, steel jacket thickness and bond strength between the steel jacket and column. For the current design jacket thickness, an increase in lateral stiffness in the range 35–60% can be expected for columns with aspect ratio of $3 \leqslant L/D \leqslant 9$. Although only a small number of ground motions were used in this study, inelastic dynamic analyses of steel-jacketed columns indicated that the jacket thickness currently specified by Caltrans provides an adequate protection against damage by the ground motions recorded during the 1989 Loma Prieta earthquake which had spectral accelerations comparable to that specified in the current design spectra. The calibration of the energy-based damage model against experiments suggested a damage index of $D_i = 0{\cdot}61$ as the repairable limit for steel jacketed columns with a jacket thickness ratio of $t_j/D = 0{\cdot}008$.

ACKNOWLEDGEMENTS

Partial support from NSF Grant CMS-94-09268 for the preparation of this paper is appreciated. Thanks are also due to Kevin Keady of Caltrans, Hans Strandgaard of CH2M Hill, Dr. R. Verma of Carter & Burgess, and Professors M.J.N. Priestley and F. Seible of University of California, San Diego, for their assistance and comments.

REFERENCES

1. Y. H. Chai, M. J. N. Priestley and F. Seible, 'Seismic retrofit of circular bridge columns for enhanced flexural performance', *ACI struct. j.* **88** (5), 572–584 (1991).
2. M. J. N. Priestley, F. Seible, Y. Xiao and R. Verma, 'Steel jacket retrofitting of reinforced concrete bridge columns for enhanced shear strength—part 2: test results and comparison with theory', *ACI struct. j.* **91**(5), 537–551 (1994).
3. G. W. Housner, Chairman of Seismic Advisory Board. 'The continuing challenge—The Northridge earthquake of January 17, 1994, '*Report to the Director, California Department of Transportation, October 1994.* The Governor's Board of Inquiry on the 1994 Northridge earthquake.
4. M. J. N. Priestley, F. Seible and C. M. Uang, 'The Northridge earthquake of January 17, 1994—damage analysis of selected freeway bridges, *Research Report SSRP-94/06,* Department of Applied Mechanics and Engineering Sciences, University of California, San Diego, La Jolla, CA 92093, February 1994.
5. J. B. Mander, M. J. N. Priestley and R. Park, 'Theoretical stress-strain model for confined concrete', *J. struct. eng. ASCE* **114**, 1804–1826 (1988).
6. Y. H. Chai, M. J. N. Priestley and F. Seible, 'Analytical model for steel jacketed R.C. circular bridge columns', *J. struct. eng. ASCE* **120**, 2358–2376 (1994).
7. Seismic Retrofit/Seismic Technology Engineering Service Center. Memo to designers memo 20–4, March 1992. Divisions of Structures, Department of Transportation, 1801, 30th Street West, M.S. 9, Sacramento, CA 95816.
8. Y. H. Chai, M. J. N. Priestley and F. Seilbe, 'Flexural retrofit of circular reinforced concrete bridge columns by steel jacketing–COLRET—a computer program for strength and ductility calculation', *Research Report No. SSRP 91-05,* Department of Applied Mechanics and Engineering Sciences, University of California, San Diego.
9. *Seismic Design References,* California Department of Transportation, Division of Structures, Sacramento, CA June 1990.
10. S. A. Mahin and J. Lin, 'Construction of inelastic response spectra for single-degree-of-freedom systems', *Research Report UCB/EERC-83/17,* Earthquake Engineering Research Center, University of California, Berkeley, CA June 1983.
11. Y. H. Chai, K. M. Romstad and S. M. Bird', Energy-based linear damage model for high-intensity seismic loading', *J. struct. eng. ASCE* **121**, 857–864 (1995).
12. Y. J. Park and A. H. S. Ang, 'Mechanistic seismic damage model for reinforced concrete', *J. struct. eng. ASCE* **111**, 722–739 (1985).
13. T. Paulay and M. J. N. Priestley, *Seismic Design of Reinforced Concrete and Masonry Buildings,* Wiley Interscience, New York, 1992.
14. Y. J. Park, A. H. S. Ang and Wen Y. K. 'Seismic damage analysis of reinforced concrete buildings', *J. struct. eng. ASCE* **111**, 740–757 (1985).